Enhanced Structural Stability of *o*-$LiMnO_2$ by Sol−Gel Coating of Al_2O_3

Jaephil Cho,*[†,‡] Yong Jeong Kim,[§]
Tae-Joon Kim,[§] and Byungwoo Park[§]

School of Materials Science and Engineering, Georgia Institute of Technology, Atlanta, Georgia 30332-0245, and School of Materials Science and Engineering, Seoul National University, Seoul, Korea

Received September 19, 2000
Revised Manuscript Received November 2, 2000

Li-ion batteries are principally the choice of power sources for portable electronics, such as cellular phones, notebook computers, and camcorders, because of their reliability, safety, and high energy density on a volume plus weight basis, compared to Ni-MH and Ni−Cd batteries. Commercial applications of batteries based upon $LiCoO_2$ cathode oxide have undergone the fastest growth since its first commercialization in 1995, and provided accepted performances, high-rate capabilities, and elevated-temperature cycling life. However, concerns related to the high cost and toxicity remain as its major drawbacks. Therefore, intensive research has been focused on lithium manganese oxide ($LiMn_2O_4$) as an alternative choice, but it shows lower discharge capacity (110−120 mAh/g) compared to $LiCoO_2$ (140−150 mAh/g).[1−5] Moreover, accelerated Mn dissolution at an elevated temperature cycling (>50 °C), and structural instability due to Jahn−Teller (J−T) distortion play key roles in diminishing the discharge capacity.[5−7] On the other hand, several recent studies have been directed to the orthorhombic $LiMnO_2$ (*o*-$LiMnO_2$) due to its high theoretical capacity.[8−14] It showed higher discharge capacities (150−170 mAh/g, depending on the C rate) than those of $LiMn_2O_4$, but the cycling performance of $LiMnO_2$ was poor at high temperature.[13] To stabilize the structural instability for elevated-temperature performance, *o*-$LiAl_{1-x}Mn_xO_2$ oxides have been studied. Their capacity retention was found to be better than that of *o*-$LiMnO_2$ by cycling tests at 55 °C with the charge and discharge current rates of 150 and 75 mA/g, respectively, between 4.4 and 2 V.[13] However, Al substitution (*o*-$LiAl_{1-x}Mn_xO_2$) decreased the original capacity of the *o*-$LiMnO_2$ cathode and did not completely prevent Jahn−Teller (J−T) distortion. As of yet, studies to prevent both structural instability and decrease of original capacity from cation substitution have not been reported in the open literature to our knowledge.

In this article, we show that sol−gel coating of Al_2O_3 on the *o*-$LiMnO_2$ particle surface can lead to the complete prevention of J−T distortion and also to the improvement of elevated-temperature stability without decreasing the capacity of the *o*-$LiMnO_2$ cathode.

Powders of *o*-$LiMnO_2$ were prepared from direct reaction of LiOH and Mn_3O_4 in a 1.05:1 mole ratio at 800 °C under N_2 atmosphere for 24 h (excess amount of Li salts was used to compensate possible Li loss). To coat Al_2O_3 on the *o*-$LiMnO_2$ powder surface (with average particle size of 13 μm), aluminum ethylhexanodiisopropoxide, $Al(OOC_7H_{15})(OC_3H_7)_2$, was first dissolved in 2-propanol, followed by continuous stirring for 20 h at 21 °C. Powders were then mixed with the coating solution such that the total amount of coating solution corresponded to 15 wt % of used *o*-$LiMnO_2$ powders. After drying the coated *o*-$LiMnO_2$ at 150 °C, it was further fired at 400 °C for 10 h under an N_2 stream. For electrochemical testing, a cathode slurry was prepared by mixing the oxide powders, carbon black (Super P), and poly(vinylidene) fluoride (PVDF) in the weight ratio 92:4:4. Coin-type cells (2016-size) contained *o*-$LiMnO_2$ oxide powders, a polyethylene microfilm separator, and a Li metal or carbon anode. The electrolyte was 1.3 M $LiPF_6$ dissolved in a mixture of ethylene carbonate/dimethyl carbonate/ethyl methyl carbonate (EC/DMC/EMC) (3/3/4 vol %).

X-ray diffraction (XRD) patterns of standard compound *o*-$LiMnO_2$ and Al_2O_3-coated *o*-$LiMnO_2$ prepared at 400 °C showed that no significant broadening of the XRD peaks of the *o*-$LiMnO_2$ was observed, while (011) diffraction peak in the orthorhombic phase was known to correlate with the planar stacking faults.[12] A full-width-at-half-maximum (fwhm) in the (011) peak was $\Delta(2\theta) = 0.096°$ (or $\Delta k = 0.0067$ Å^{-1}, where $k = (4\pi/\lambda) \sin\theta$ is the scattering vector). It shows that the present material has a relatively well-ordered orthorhombic structure (*Pnmn*). However, the XRD pattern of the coated oxide was apparently similar to that of the uncoated oxide. This is possibly due to formation of a thin Al_2O_3 coating layer or of *o*-$LiMn_{1-x}Al_xO_2$ solid solution near the surface as a result of reaction between Al_2O_3 and *o*-$LiMnO_2$.

To examine the distribution of Al atoms near the particle surface, an electron probe mass analysis (EPMA) in the coated *o*-$LiMnO_2$ was carried out from a cross section of polished powders (Figure 1). The result shows that a significant amount of Al atoms corresponding to approximately 30 atom % is observed within the 2 μm range in the vicinity of the surface, indicating the

---

* Corresponding author.

[†] On leave from Samsung SDI Co., Ltd, Chonan, Chungchongnam-Do, Korea.

[‡] Georgia Institute of Technology.

[§] Seoul National University.

(1) Thackeray, M. M.; David, W. I. F.; Burce, P. G.; Goodenough, J. B. *Mater. Res. Bull.* **1983**, *18*, 461.
(2) Thackeray, M. M.; Johnson, P. J.; de Picciotto, L. A.; Bruce, P. G.; Goodenough, J. B. *Mater. Res. Bull.* **1984**, *19*, 179.
(3) Gummow, R. J.; de Kock, A.; Thackeray, M. M. *Solid State Ionics* **1990**, *69*, 59.
(4) Cho, J.; Thackeray, M. M. *J. Electrochem. Soc.* **1999**, *146*, 3577.
(5) Amatucci, G. G.; Schmutz, C. N.; Blyr, A.; Sigala, C.; Gozdz, A. S.; Larcher, D.; Tarascon, J. M. *J. Power Sources* **1997**, *69*, 11.
(6) de Kock, A.; Rossouw, M. H.; de Picciotto, L. A.; Thackeray, M. M.; David, W. I. F.; Hull, S. A. *Mater. Res. Bull.* **1990**, *25*, 657.
(7) Cho, J. *Solid State Ionics*, in press.
(8) Shu, Z. X.; Davidson, I. J.; McMillan, R. S.; Murray, J. J. *J. Power Sources* **1995**, *54*, 232.
(9) Vitins, G.; West, K. *J. Electrochem. Soc.* **1997**, *144*, 2587.
(10) Gummow, R. J.; Thackeray, M. M. *J. Electrochem. Soc.* **1994**, *141*, 1178.
(11) Ohzuku, T.; Ueda, A.; Hirai, T. *Chem. Express* **1992**, *7*, 193.
(12) Croguennec, L.; Deniard, P.; Brec, R.; Lecerf, A. *J. Mater. Chem.* **1997**, *7*, 511.
(13) Chiang, Y.; Sadoway, D. R.; Jang, Y.; Huang, B.; Wang, H. *Electrochem. Solid State Lett.* **1999**, *2*, 107.
(14) Tang, W.; Kanoh, H.; Ooi, K. *J. Solid State Chem.* **1999**, *142*, 19.

10.1021/cm000759+ CCC: $20.00

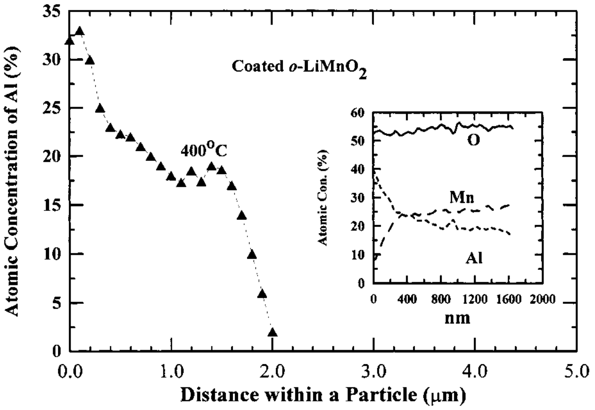

Figure 1. EPMA profile of Al concentration near the particle surface. The inset is an AES of O, Al, and Mn atoms in the coated o-$LiMnO_2$ powder prepared at 400 °C.

formation of the solid solution. This EPMA result is consistent with that of Auger electron spectroscopy (AES) analysis (shown as an inset in Figure 1). The thickness of the solid solution region is estimated to be on the order of 1 μm, where a sputtering rate of 260 Å/min obtained from a standard SiO_2 is assumed to be the sputtering rate of the present sample. Even such a high concentration of Al atoms at the surface within ~1 μm did not affect the overall lattice parameters. The lattice constants a, b, and c of bare o-$LiMnO_2$ are 2.806 ± 0.012 Å, 5.756 ± 0.011 Å, and 4.572 ± 0.014 Å, respectively, while those of the Al_2O_3-coated oxide prepared at 400 °C are 2.803 ± 0.014 Å, 5.755 ± 0.015 Å, and 4.579 ± 0.018 Å, respectively. Another interesting observation in the coated o-$LiMnO_2$ prepared at 400 °C is the disappearance of the Li_2MnO_3 phase, as confirmed from XRD analysis. This is likely to indicate that the second phase (Li_2MnO_3) is distributed in the vicinity of the bare-$LiMnO_2$ surface. However, during Al_2O_3 coating by 400 °C heat treatment, the second phase (Li_2MnO_3) reacts with Al_2O_3, probably decomposing into $LiMnO_2$ and $LiAlO_2$.

A plot of the voltage profile of a typical o-$LiMnO_2$ cell after seven cycles at 0.2 C rate (=36 mA/g) between 4.5 and 2 V at 55 °C is shown in Figure 2a, and well-developed plateaus at 3 and 4 V are observed. The lithium ions in $Li_xMn_2O_4$ remain on the 8a tetragonal sites within a cubic structure for the range $0 < x \leq 1$; this reaction occurs at approximately 4 V versus lithium metal.[1,2] On the other hand, insertion of lithium into $Li_xMn_2O_4$ occurs at 3 V for $1 < x \leq 2$;[1] it causes a first-order phase transition to rock salt phase $Li_2Mn_2O_4$ during which the tetrahedrally coordinated lithium ions are cooperatively displaced into the octahedral sites (16c). The capacity versus cycle numbers of both kinds of cells have been measured up to 50 times, as shown in Figure 2b. After seven cycles, the discharge capacity of the coated o-$LiMnO_2$ becomes similar to that of bare oxide, showing 170 mAh/g. However, it shows only 2% capacity loss after 50 cycles, which is superior to that of the bare one (35% loss) in its capacity stability. Even though $LiMn_{1-x}Al_xO_2$ formation at the surface decreases the overall capacity of coated oxide initially, its capacity rapidly increases after further cycling. This behavior may be due to the formation of disordered solid solution at the surface from low coating temperature. A more detailed study is in progress to investigate the degree of crystallinity of the solid solution at the oxide particle.

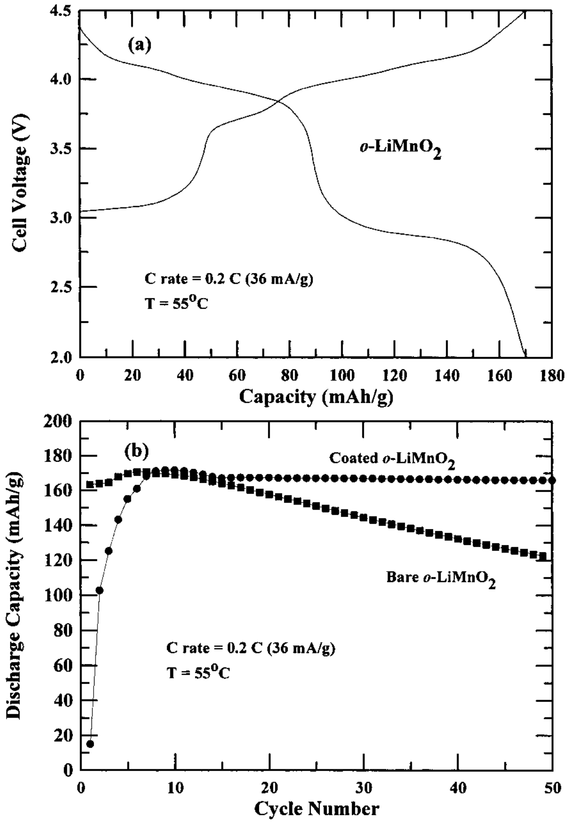

Figure 2. (a) Voltage profiles of typical o-$LIMnO_2$ oxide after 10 cycles in a $Li/LiMnO_2$ cell and (b) plot of discharge capacity of the bare and coated o-$LiMnO_2$ versus number of cycles at 0.2 C rate between 2 and 4.5 V.

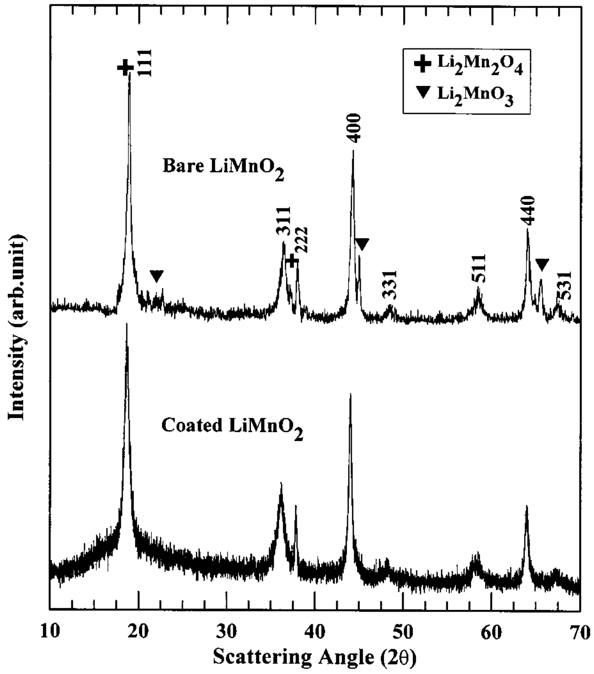

Figure 3. XRD patterns of uncoated and coated o-$LiMnO_2$ electrode, discharged to 2 V after 50 cycles.

To understand the origin of the superior stability of the coated o-$LiMnO_2$ compared to the bare one, XRD patterns of 50 cycled cells discharged to 2 V were compared in Figure 3. The XRD pattern of the bare *o*-$LiMnO_2$ electrode shows minor $Li_2Mn_2O_4$ and Li_2MnO_3 phases, but those totally disappeared in that of the coated electrode. An entire disappearance of the strongest (010) peak in *o*-$LiMnO_2$ at 15.4° indicates the disappearance of the orthorhombic phase in the cycled *o*-$LiMnO_2$ electrode. Appearance of the cubic phase in the bare and coated *o*-$LiMnO_2$ electrodes is evident for a cycling-induced phase transformation. The XRD patterns of the uncoated oxides show small peaks at about 18.6° and 65.5°, indicating a trace amount of Li_2MnO_3 in the parent compound, but the overall intensities of those peaks appear to grow after cycling. This was reported to be due to the dissolution of only MnO from $Li_2Mn_2O_4$ ($Li_2Mn_2O_4 \rightarrow MnO + Li_2MnO_3$).[4] The dissolution of MnO into electrolyte results in an increase in Li:Mn ratio in the residual structure and a concomitant oxidation of Mn^{3+} to Mn^{4+}. Note that the XRD pattern of the bare *o*-$LiMnO_2$ electrode in the fully lithiated state (Figure 3) appears to be predominantly a cubic spinel, while lithiation of $LiMn_2O_4$ shows the tetragonal spinel phase. The collective J−T distortion occurs at an average Mn valence below 3.5, and cycling fading of the spinels has been attributed from this distortion.[1,2] The XRD pattern of the coated electrode indicates that the J−T distortion is totally suppressed by the Al_2O_3 coating. The results imply that the protective coating layer can prevent the Mn dissolution from the manganese spinel and also prevents lattice instability resulting from the J−T distortion.

CM000759+